Nanocrystalline Ni-Cu Electroplated Alloys Cathodes for Hydrogen Generation in Phosphate-Buffered neutral electrolyte

Mosaad Negem[a*], H. Nady, and C.W.Dunnill[b*]

[a]Chemistry Department, Faculty of Science, Fayoum University, Fayoum, Egypt

[b]Energy Safety Research Institute (ESRI), Swansea University Bay Campus, Swansea SA1 8EN, United Kingdom

Abstract

The use of hydrogen as a green fuel alongside an environmentally friendly electrolyte is the most promising technology required for the conversion and storage of renewable energies and the transition to a low carbon future. Current electrolyte solutions include strong acid and bases but few are phosphate buffered neutral electrolyte (PBNE) in pH with significant advances in the application associated with a PBNE and benign electrolyte solution. Nanocrystalline Ni-Cu alloys have been electroplated onto copper electrodes and characterized via scanning electron microscopy (SEM), energy dispersive X-ray spectroscopy (EDX) and X-ray diffraction, XRD. The Electrocatalytic performance of the electroplated Ni-Cu alloys cathodes for the hydrogen evolution reaction (HER) was assessed by cyclic voltammetry (CV), electrochemical impedance spectroscopy (EIS) and cathodic polarization measurements in a PBNE. The results demonstrate that the nanocrystalline Ni-Cu alloys cathodes have high electrocatalytic efficiency for HER. The electrocatalytic activity of the electroplated Ni-Cu alloys depends on the morphology, size and synergistic effect of Ni and Cu. The most active cathode was found to be a 30:70 ratio alloy of Ni:Cu in the PBNE and had twice the intrinsic electrocatalytic activity than the pure nickel and 1.5 times higher than standard Pt/C in PBNE at potential -2.0 V. The overpotential of HER required to reach a catalytic current density of 10.0 mA/cm^2 was 284 mV vs. RHE. The nanocrystalline 30:70 alloy exhibits the highest intrinsic activity towards the HER and can be

applied as a cathode for H_2 production in the industrial water electrolyzer, potentially increasing the efficiency of devices and thus lowering the cost of green hydrogen production.

Keywords:

Ni-Cu Alloys; Electrocatalyst; HER; EIS, Nanocrystalline cathode; Ultrasound; Polarization
Corresponding author: mra00@fayoum.edu.eg (Mosaad Negem) * Tel: 00201112278865
c.dunnill@swansea.ac.uk (Charles Dunnill).

1. Introduction

Climate change resulting from the huge consumption of fossil fuel generating CO_2 and other harmful gases is already having effects on global weather patterns and will likely have a catastrophic effect on our continued existence on the planet in generations to come. Splitting water electrochemically is a sustainable technology to produce renewable and green hydrogen which is a sustainable fuel. Hydrogen is the most abundant element on the earth and when produced from renewable energy and water is able to substitute conventional fossil fuel use or employed in various applications including fuel cells to produce electrical energy. Renewable energy sources, wind, solar, tidal, wave etc. tend to be intermittent, requiring a storage capacity that is able to de-couple supply from the demand which can be achieved through the electrolysis of water and th4 production of green hydrogen as well as significant advantages in transporting the energy for use on demand. The electrocatalysts which attain considerable electrocatalytic activity to produce electrochemically hydrogen with high efficiency via water electrolysis have great attention to supersede expensive noble metals electrocatalysts such as Pt. Moreover, the electrolysis of water implemented to generate green hydrogen via PBNE is considered to be additionally clean and effective no corrosive solutions are needed in the process. The stable, cost-effective and efficient electrocatalyst for HER in PBNE is necessary due to the problem of corrosion specifically in harsh acidic and alkaline electrolytes to protect the environment. The

use of Ni-based cathodes can dramatically lessen the cost of the electrocatalyst in case of the corrosion resistance of these cathodes improved. The PBNE is the ultimate ideal solvent for water splitting. The stability of the electrolytes such H_2SO_4, KOH or PBNE during the HER is crucial factor due to the continuous change of the pH of the electrolyte affecting greatly the efficiency of this process. The change of electrolyte pH leads to varying in electrolyte conductance and generally in the order H_2SO_4 > KOH > PBNE [1]. Therefore, PBNE is considered the most suitable electrolyte for HER. Nonetheless, little research has been performed on HER in PBNE or near-neutral which attain various advantages like eco-affable, high catalyst stability, non-corrosive and safety. We report here the high activity of nanocrystalline Ni-Cu alloys to generate hydrogen from PBNE with higher efficiency than observed in alkaline medium[2]. Long term, the electrolysis of ocean or river water using PBNE is the essential objective to satisfy a reliable future hydrogen economy[3].

M-H bond strength greatly influences the electrocatalytic efficiency of the electrocatalyst towards HER via change of adsorption and desorption of reactant and product which is considered a critical parameter for these processes[4]. There is a correlation between HER activity and the energy of H adsorption onto a single transition metal like Mo, Co, Ni, and W which possess stronger hydrogen adsorption but the more noble metals such as Cu, Ag, and Au attain frail adsorption of hydrogen[5]. The M-H bond strength can be adjusted via a combination of more than one metal such as Cu and Ni which form the stable combination in PBNE. Adsorption of H on the copper surface is very weak while Ni possesses the high adsorption properties of H, which can slow the HER[6]. The combination of Ni and Cu produces new cathodes with adjustable M-H bond strength which have a high rate of HER in acidic and alkaline electrolytes[7,8],[9].

The sustainability of the cathode materials is contingent upon energy consumption, their stability throughout the electrolysis process, and electrocatalysis activity minimising ohmic resistance and an enhanced lifetime of cathode papers [10][11][12]. Moreover, the electrocatalysis activity of the cathode materials can be developed through the synergetic combination of the electrocatalytic constituents, the number of active sites, and their surface area using electroplating[13]. Ni alloys possess recognized electrocatalytic activity towards the HER and the numerous electrochemical processes[7,14–16][12]. Ni-based alloys are distinguished with their chemical stabilities in aggressive electrolytes, appropriate mechanical properties, and inexpensive materials. Moreover, Ni-based alloys have enhanced electrocatalytic activity which can diminish the energy barrier of HER[17]. Ni acquires a high electrocatalysis activity to the HER generation that can be boosted via combination by appropriate metal due to the electrocatalytic synergistic influence well described in the literature[18]. The electrocatalysis efficiency of Ni cathode can be developed by combining with transition metal like Co, V, W, Mo, Cu, and Zn by electroplating[8,15,26,27,16,19–25][12]. The electroplating can change the crystal lattice system, chemical composition, and size of unit cell producing the significant surface area, large numbers of active sites, and new electronic structure. The activation energy of the HER can be diminished by adding transition-metal changing the electrode reaction mechanism.[28] In addition, electroplating conditions influence the chemical and physical characteristics of the Ni-based alloys materials that can improve the electrocatalysis activity with regard to the HER. The high electrocatalysis efficiency of HER attained via Ni-based alloys in the PBNE directs to the promising applications of these materials to produce hydrogen in the industry. Furthermore, Ni-Cu alloys possess high resistance to corrosion and superior stability[29]. Nevertheless, the electroplated Ni-Cu alloys have no report to examine their

electrocatalysis efficiency toward the HER in PBNE. In this research, the electrocatalysis kinetics of nanocrystalline Ni-Cu alloys electroplated from sulphate-gluconate using ultrasonication conditions and galvanostatic technique for HER. The hydrogen evolution reaction has been investigated in PBNE by electrochemical impedance spectroscopy, cyclic voltammetry, and cathodic polarization in PBNE to the possible application as electrocatalysts in hydrogen generation.

2. Experimental

2.1 Alloys preparation and material characterization

The highly homogenous Ni-Cu alloys have been electroplated on Cu foil utilized as a cathode with Pt sheets used as anode with a surface area of 2.4 cm^2. The electroplating of the nanocrystalline Ni-Cu alloys materials has been implemented via the cylindrical Pyrex cell and TTI / PL310 (32V-1A PSU) has generated the direct current. The ultrasonic bath of Branson 3510 (power 100 W- frequency 42 kHz) has been operated to generate the ultrasonic waves into the electroplating cell. The conductivity and pH of the electroplating electrolytes have been obtained using Mettler Toledo. The electroplating electrolytes have been prepared using $NiSO_4.7H_2O$, H_3BO_3, $CuSO_4.5H_2O$, cysteine and sodium gluconate bought from Aldrich, Sigma and Merck. The electroplating electrolytes have been obtained via weighing and dissolving in deionized water to create the required concentrations. The nanocrystalline Ni-Cu alloys materials have been prepared via the gluconate bath under current density, 2.5 Adm^{-2} at pH=4. The electroplating process has been implemented for 1 h at 293 K onto the foil of copper. Various concentrations of the additives such as complexing agent and cysteine have been utilized to optimize the conditions of Ni-Cu alloys materials electroplating. The newly prepared electrolyte has been used for each electroplating experiment. The copper foil has been etched chemically

using HNO_3 1:1 for 1 min to eliminate the native copper oxide layer, bathed with deionized water, and finally washed via acetone and weighted. The morphological structure and elemental composition of the Ni-Cu alloys materials have been investigated via a scanning electron microscope, SEM, JOEL JSM-5300 LV/ 25 kV and a high vacuum and energy dispersive X-ray analysis which was fitted with SEM and the data are presented in Table 2. In addition, the crystalline lattice system of Ni-Cu alloys has been characterized via X-ray diffraction, XRD.

2.2 Electrochemical measurements

The electrochemical cell was a conventional all-glass three electrodes including Pt utilized as counter electrode and saturated calomel electrode operated as a reference electrode. The electrochemical investigations have been implemented using the aqueous electrolytes, analytical grade reagents, and deionized water. A PBNE of 1.0 M has been freshly prepared to study the electrocatalytic activity of Ni-Cu alloys towards the HER. The potentiodynamic polarization and electrochemical impedance spectroscopy (EIS) surveys have been performed via a Voltalab PGZ 100. The potential has been scrutinized versus a saturated calomel electrode, 0.245 V vs. the standard hydrogen electrode, SHE. The potentiodynamic polarization investigations have been fulfilled via the scan rate of 5 mV s^{-1} to reach the quasi-stationary condition. The impedance (Z) and phase shift (Θ) have been chronicled through the frequency domain of 0.1-10^5 Hz. The superimposed ac-signal was 10 mV peak to peak. To obtain reproducibility, each experiment has been accomplished at least twice.

3. Results and discussion

3.1 Structure, composition and Electrochemical properties electrodeposited alloys

Various Ni-Cu_x alloys (x =19, 24, 26, 27, 44, 49, 59, 70, 86 and 94 at % Cu) have electroplated as nanocrystalline film on Cu foil substrate. It is necessary to scrutinize the morphological structure, crystal lattice system and the elemental components of the electroplated

cathodes. The SEM images of Fig. 1a, b, and c display clearly that the electroplating of nanocrystalline Ni-Cu alloys via the gluconate-cysteine baths and the conventional ultrasonication, CUW, is appropriate and simple to manage. The employment of cysteine and gluconate salt, as well as boric acid, develops the morphological structure of the nanocrystalline Ni-Cu alloys. Such combination leads to shiny and mesoporous granular structure of Ni-Cu alloys producing huge active surface area for HER. In addition, the influence of cysteine creates the dense, smooth and shiny Ni film at different current density changed between 0.05 and 10 Adm^{-2}. Furthermore, it was found that the morphological structure of electroplated Ni has been slightly influenced via the escalation of the current densities across 0.1 -12 Adm^{-2} under the CUW. Figure 1 exhibits the SEM images of the nanocrystalline Ni-Cu alloys electroplated via gluconate bath and a current density of 2.5 Adm^{-2}. Nevertheless, the use of high current density further than 2.5 Adm^{-2} produced very rough layers of Ni-Cu alloys. The morphology of Ni-23.84Cu alloy is flower-like structure while Ni-44.46Cu and Ni-58.78Cu alloys are rounded grains. The EDX spectra of Ni-Cu alloys are merged in the same Fig. 1. The relative atomic ratios of Ni and Cu for the electroplated alloys as attained via the EDX analysis are shown in Figure 1.

Fig. 2 displays the XRD patterns acquired for nanocrystalline Ni-Cu alloys with different compositions that assembled in the face centred cubic of space group with JCPDS number 351360 and the height peak of (111) facet enlarged with increase Cu%. The unit cell parameters of Ni-Cu alloys vary between a = 2.033 Å and a = 2.083 Å with an increase Cu%. The XRD patterns of the electroplated Ni-Cu alloys confirm that the intensities of the peaks related to nanograins have been obtained. The average grain sizes of the nanocrystalline Ni-Cu alloys have

been calculated via Debye-Scherer's equation and the XRD patterns. The average grain size of nanocrystalline Ni-Cu alloys enlarged with Cu% from 15 nm to 90 nm.

2.2.Cyclic voltammetry of different electrodes

The electrochemical behaviour of the different electroplated cathodes has been scrutinized in 1.0 M PBNE and related cyclic voltammogram, CVs, have been exhibited in **Fig. 3a** and **b**. For the comparison, CV of pure Cu and Ni electrodes has been investigated under the same conditions. Pure Ni and pure Cu possess their own characteristic redox peak. A typical CV of pure Ni over the same electrolyte is shown in **Fig. 3a**. The potential scan has been initiated at -7.0 V, where a significant cathodic current density has been observed attributable to HER. Starting a positive- progressing sweep where the cathodic current density is lessened as the potential is moved to less negative values. There is then the active region with respect to metal dissolution, in which the current density is increased with potential. On the anodic extent, oxidation peak originates at about -0.5 V ensued via active anodic dissolution till -0.05 V. It was described that the principally soluble Ni species in a PBNE were either $Ni(OH)^{+}_{(aq)}$ or $Ni^{2+}_{(aq)}$ [30,31]. The dissolution of Ni was reported to be pH-dependent, which suggests a contribution of OH^- towards the active dissolution reaction [30]. Respecting the reliance of the active current density via OH^- concentration in the electrolytes, the entire anodic dissolution mechanisms can be represented through: $Ni + OH^- = Ni(OH)_{ads} + e^-$, $Ni + H_2O = Ni(OH)_{ads} + H^+ + e^-$ and $Ni(OH)_{ads} = Ni(OH)^{+}_{aq} + e^-$. Ni can be passivated via forming a thin layer of $Ni(OH)_2$ and possibly NiO onto the metal surface in PBNE as the ensuing reactions: $Ni(OH)_{ads} + OH^- = Ni(OH)_2 + e^-$, $Ni(OH)_{ads} + H_2O = Ni(OH)_2 + H^+ + e^-$ and $Ni(OH)_2 = NiO + H_2O$ [32] . Consequently, a layer of $Ni(OH)_2$ or NiO is deposited on the metal surface which possesses the recorded region of passivation where the current density becomes stable with increasing potential. The reverse scan of the potential has no cathodic peak pertaining to the reduction of

the $Ni(OH)_2$ or NiO passive film. This involves a considerable cathodic current attained attributable to hydrogen evolution reaction.

The CV for electroplated Cu was recorded in PBS and presented in Fig. 3a. During commencing the potential scan at −7.0 V, low cathodic current density is recorded possibly due to the formation of adsorbed species on the Cu surface like Cu $(H_2O)_{ads}$ and/or Cu $(OH)^-_{ads}$ [33]: $Cu + H_2O = Cu(H_2O)_{ads}$ and $Cu + OH^- = Cu(OH)^-_{ads}$. In the anodic active area, Cu suffers from the dissolution into the solution like Cu^+ ions and the current density is unceasingly increased with potential[33]. The increase in the anodic current density is due to the dissolution of metal at the surface and formation of Cu^+ ions. The anodic peak is ascribed to a dissolution/passivation process that happens in the following way: (a) Dissolution of the adsorbed layer consistent with: $Cu(H_2O)_{ads} + OH^- = Cu(OH)^-_{2(aq)} + H^+ + e^-$ and $Cu(OH)^-_{ads} + OH^- = Cu(OH)^-_{2(aq)} + e^-$. (b) The development of a passive film, Cu_2O, in accordance with [34]: $2Cu(OH)^-_{2(aq)} = Cu_2O + H_2O + 2OH^-$ and $2Cu(OH)^-_{ads} = Cu_2O + H_2O + 2e^-$. The anodic peak is due to the oxidation of the outer layer of the oxide film, Cu_2O, at the oxide/solution interface into Cu(II) oxide or a hydroxide according to: $Cu_2O + H_2O = 2CuO + 2H^+ + 2e^-$ and $Cu_2O + 3H_2O = 2Cu(OH)_2 + 2H^+ + 2e^-$. The development of the CuO layer clarifies the decrease of the anodic current density, which can be perceived by an obvious peak. The redox peak of Ni-Cu alloys situates in between that of pure metals (Ni and Cu), but the shape is related to the characteristic peak location of pure Cu. In addition, the Ni content has no great effect on the number and the site of an anodic peak which demonstrates that the kinetic processes are dominated by the dissolution of Cu. The values of the anodic current density decline with the increase of the Cu content in the alloys which indicates the increase of the stability of Ni-Cu alloys and high corrosion resistance with an increase of Cu in PBNE. This is due to the formation of a doped oxide/hydroxide layer on the surface of the

alloy. The doped oxide/hydroxide layer of Ni/Cu protects the Ni-Cu alloys from the continuous dissolution into the PBNE during HER. This confirms that the Ni-Cu alloys possess high and long stability in the PBNE which are the most promising materials for the HER in this electrolyte.

3.3. Electrocatalytic activity of the electroplated cathodes towards HER

3.3.1 Polarization measurements

The significant aim of the present work is to utilize the nanocrystalline Ni-Cu alloys for HER within phosphate-buffered neutral environments. To evaluate the HER catalytic activity of the nanocrystalline Ni-Cu alloys in PBNE, the three-electrodes system in 1.0 M PBNE have been established. Electrocatalytic activity of the Ni-Cu alloys cathodes for HER was investigated by cathodic polarization and EIS measurements. To determine the electrocatalytic activity of the electroplated Ni-Cu alloys, the cathodic polarization measurements have been performed to compare between ed. Ni, bulk Ni, ed. Cu and Pt/C cathodes and the electroplated Ni-Cu alloys as shown in **Fig. 4a**. As can be seen in Fig. 4a, bulk electrodes (Ni or Cu) display lower performance for the HER than electroplated nanomaterials. This result suggests that the electrocatalytic activity of the HER emanates mainly from the surface structure, crystal lattice system and synergistic effect of the electrocatalyst. The cathodic overpotential of hydrogen on the cathodes is an important parameter that controls the HER and determines the rate of H_2 evolution, presented as the recorded cathodic current density at the same potential. The cathodic overpotential of hydrogen provides a comparison factor to determine the electrocatalytic activity of the investigated cathodes. Therefore, the activity of the hydrogen evolution via different cathodes is obtained by determination of the overpotential of HER at 10 and 100 mA cm^{-2} and the hydrogen evolution current density at -1.1 V SCE which have been recorded and presented in

Table 1. The electrocatalytic activity of the electroplated Ni-Cu alloys towards the HER is clear, and the evolution potential of H_2 on these alloys cathodes is more positive than that of bulk electrodes (*cf.* Fig. 4a). This means that the nanograins and synergistic effect of the electroplated materials augment the electrocatalytic activity of the cathodes towards the HER. The cathodic current-potential curves of the nanocrystalline Ni-Cu electrocatalysts with different Cu content which are obtained in 1.0M PBS solution are given in the same Fig. 4a. The increase of the Cu content up to ≈ 70% lessens the cathodic hydrogen overpotential, η_{10} (*Cf.* Table 1 and Fig. 4b) then increased again. From Fig. 4b, it can be recommended that the hydrogen evolution on Ni-Cu cathode increases with increasing the Cu content and a rapid boost in the current with growing applied voltage because of the evolution of H_2 at the cathode (*Cf.* Table 1 and Fig. 4a). By plotting current densities recorded at a potential of -1.1 V (*vs.* SCE) as shown in Fig. 4b, it can be found that Ni-70Cu cathode has a maximized current density of 77.2 mA cm^{-2} compared with the other considered cathodes. Moreover, the catalytic current density of the Ni-70Cu electrode is higher than standard Pt/C by 1.5 times in PBNE at potential -2.0 V. Therefore, the high catalytic performances and most cost effectiveness makes the Ni-70Cu cathode the most promising for HER process in the PBNE. From the presented polarization data, it is clear that the developed coatings yield remarkably high HER catalytic activity, and the Ni-70Cu layer possesses the highest current density and lowest overpotential. Also, the Ni-70Cu cathode attains a relatively more positive hydrogen overpotential (Cf, Table 3) compared to the other Ni-Cu alloys cathodes, indicating that the 70% Cu content alloy enhances the electrocatalytic activity of electroplated Ni-Cu electrodes towards the HER, which is beneficial for electrochemical H_2 production in PBNE environments. It is evident that different mesopores are clearly attained in all electroplated Ni-Cu cathodes. Many mesopores are found on the electrodes prepared from the

≈ 70% Cu alloy which attain huge surface area with a large number of active surface sites, developing an electron transfer pathway. The possessing of these mesopores and valleys is essential for superior utilization of Raney nickel to elctrocatalyse HER. The mesopores and valleys filled with the PBNE, containing a considerable space of the internal surface of the Raney nickel, accessible to electrochemical H_2 evolution reactions. Plentiful mesopores and valleys obtained in Ni-70Cu cathode produce adequately diminutive diffusion paths of dissolved hydrogen, for the most rapid release of the gas and preclude unnecessary gathering of the hydrogen gas and concentration polarization in the mesopores[35]. It is known that the adsorption of H onto Cu is so feeble which decelerate the reduction reaction of H^+ while Ni possesses the high that the adsorption of H which lessens the release of H_2[36]. Mixing of Ni and Cu is successfully creating a moderate H adsorption strength properties at the active sites which enhances H_2 evolution. The auspicious electrocatalyst must attain the lowest adsorption free energy of the hydrogen, water, and its components in accordance with Sabatier's principle $\Delta G \approx 0$, d band in the bridge Fermi level and has the uppermost electron[37]. The electrocatalysts possess the considerable interaction concerning its d-band and 1s orbital of hydrogen is notably active for the HER [37] which can be implemented by homogenously doping Ni by an element such as Cu. Moreover, the electrocatalytic activity of the Ni-Cu alloys is greatly influenced via the synergetic effect between the physical and chemical characteristics of these alloys. Therefore, electrocatalysis is influenced by the nature of the material in terms of the morphological structure of the cathode surface. Essentially, the cathodic hydrogen evolution reaction proceeds via four steps beginning by a discharge of hydrogen ions and is finished via the release of the molecular hydrogen. The rate determining step may be either one of these four steps which is responsible for the existence of HER overpotential. At the same time, it is imperative to recognize that

electrocatalysis for any electrochemical reaction is attributable to presence of active surface sites, which permit the easy transfer of the electrons.

To determine the HER kinetics of the investigated catalysts and the rate-determining step of the HER, Tafel plots derived from the corresponding polarization curves are presented in Fig. 4c. The Tafel slops of bulk Ni, ed. Ni, ed. Cu, Ni-24Cu, Ni-59Cu, Ni-70Cu and Ni-85Cu are 123, 114, 133, 149, 138, 109 and 116 mV dec^{-1}, respectively. In general, the HER could proceed through either a Volmer–Tafel or Volmer–Heyrovsky mechanism.[38] According to two-electron-reaction model, electrocatalytic HER proceeds in the two steps: The first step is the discharge step (Volmer reaction: $H_2O + e^- \rightarrow H_{ads} + OH^-$, 116 mV dec^{-1}) and the second step can pass through two pathway (electrochemical desorption step, Heyrovsky reaction: $H_{ads} + H_2O + e^- \rightarrow H_2 + OH^-$, 40 mV dec^{-1}) and recombination step (Tafel reaction: $2H_{ads} \rightarrow H_2$, 30 mV dec^{-1})]. [39]According to the b_c values, the H_2 evolution on Ni-Cu electrodes is controlled by the Volmer-Heyrovsky HER mechanism ($H_2O + e^- \rightarrow H_{ads} + OH^-$; $H_{ads} + H_2O + e^- \rightarrow H_2 + OH^-$,), in which the discharge reaction is fast and H_2 is evolved by a rate-determining ion and atom reaction. Among all the electrodes, Ni-70Cu coating shows the lowest slope values; this indicates better H_2 evolution activity and fast proton discharge kinetics at this electrode. As listed in Table 2, this HER performance makes the Ni-70Cu coating electrode comparable or smaller than that of other reported as HER electrocatalysts in different media[40,41,50–57,42–49] .The better HER activity of Ni-70Cu catalyst relative to the other catalysts could mostly be correlated with not only its morphology but also a proper composition. Fig. 4d shows that the high electrocatalytic activity of Ni-70Cu alloys in PBNE than alkaline medium. This confirms that the Ni-Cu alloys are most auspicious electrocatalysts for HER using PBNE in the industry.

3.3.2 Electrochemical impedance spectroscopy, EIS.

EIS is an influential technique to investigate the electrode-electrolyte interface and frequently implemented to study the H_2 evolution reaction.[27] Charge transfer manipulated, diffusion influenced and combined kinetics phenomena can be precisely characterized via this method. With the purpose of stipulating a physical picture of a cathode/electrolyte interface and the electrochemical processes happening at a cathode surface, experimental EIS results have been modelled via Z fit analysis software offered with the impedance system. EIS has been used to investigate the properties of electrode/solution interface, electrochemical reaction and electron transfer kinetics of Ni-Cu alloys cathodes during the HER processes. The attained EIS data elucidate the electrochemical processes developed at an interface of the cathode- electrolyte. The impedance data of electroplated Ni, Cu, and Ni-70Cu layers are presented as Nyquist plots in **Fig. 5** to evaluate the efficiency of the Ni, Cu and Ni-70Cu cathodes towards the electrocatalytic hydrogen evolution reaction. The data has been recorded at a constant cathodic potential of -1.0 V during H_2 generated at an appreciable rate. The complex-plane impedance curves of the Ni, Cu and Ni-Cu cathodes exhibit two capacitive loops which are characteristic behaviour of a mesoporous surface.[58] The first one is observed at high frequencies with a diameter (resistance) R_1 and the second one is remarked throughout the medium- and low-frequency domains and high resistance, R_2. The impedance responses of the Ni-Cu electrocatalysts were fitted by the equivalent circuit presented in **Fig. 5(inset)**, where the overall impedance of alloys cathodes is exemplified by a parallel association of capacitance and resistance of the two charge-transfer processes. The scatterings at small frequencies for the activated cathodes can be probably owing to the variability of impedance and active hydrogen bubble evolution. The entire charge-transfer resistance, R_f, equates (R_1 + R_2). The circuit constituents (C_1 /R_1) and (C_2 / R_2) are correlated to the high- and low- frequency capacitive hoops, respectively.[26] From Fig. 5

the impedance values of the electroplated Ni-70Cu alloy electrode are considerably lower than those recorded for pure elements (Ni and Cu), which signifies a dissimilar nature of the HER on the electroplated alloys and pure elements. The fitting parameters of the impedance results are recorded in **Table 3**. A charge-transfer resistance determines the information concerning the rate of the electrochemical reaction like HER where the lowest value of the charge-transfer resistance obtained by the electrocatalyst delivers the highest rate of HER. The charge-transfer resistance which is the ideal circumstance can be identified as semicircle diameter corresponding to impedance data.[59] **Table 3** shows clearly how the entire charge-transfer resistance, R_f, for the HER on the electroplated Ni-70Cu alloy cathodes is significantly lower than that obtained by the electroplated Ni, Ni-Cu alloys and Cu cathodes. This can be attributed to the morphology, nanosize of grains, adjustable adsorption free energy of hydrogen, and synergistic and intrinsic effect acquired via the Ni-70Cu alloy which lead to the highly active site for the electrocatalysis processes. A comparison of the intrinsic electrocatalytic activity implies that an increase in the activity of different compositions of Ni-Cu alloys cathodes develops from a change in electronic structure, unit cell parameters, morphology and the surface roughness obtained via the Cu-enriched alloys layer. In addition, the principal difference of the intrinsic electrocatalytic activity is correlated to the variations in a charge transfer coefficient[60]. Because the surface roughness increases rapidly with an increase in Cu%, it implies that the intrinsic electrocatalytic activity of the Ni-Cu alloys increases with the copper contents. This confirms that the intrinsic electrocatalytic activity of the Ni-Cu alloys is responsible for the enhancement of the activity towards HER. In fact, it can be seen that the electroplated Ni–70Cu alloy cathode is a more efficient catalyst for the HER.

EIS measurements at various cathodic potentials were performed to elucidate the effect of cathodic polarization on the behaviour of the electroplated layers during the HER. **Fig. 6** presents the EIS curves attained for the electroplated Ni-70Cu cathode in 1M PBS at the various cathodic potentials, namely, -1.0, -1.05, -1.1, -1.2, -1.3, -1.4, and -1.5 V vs. SCE. The EIS experimental results attained for the Ni-Cu cathodes have been fitted to theoretical data consistent with the model of an equivalent circuit which is displayed as an inset into Fig. 5. The EIS data of Ni-70Cu cathode displays the characteristic behaviour of adjustable electronic structure and the small unit cell obtained in electroplated Ni-Cu cathode to electrocatalyse the hydrogen evolution reaction. The calculated values at different potentials are exhibited in **Table 3**. It is recognizable that, the two-time constants responses are clearly existent at all cathodic potentials, which demonstrate the formation of two partly overlapping semicircles, with the high-frequency semicircle correlated to the mesoporous morphology of a cathode and the low-frequency semicircle. The two peaks have been perceived across the phase angle-frequency plots which conform the two semicircles obtained in impedance measurements. The change of the R_f throughout the shift of cathodic potential for the Ni-70Cu cathode is exposed in **Fig. 6a(inset)** which confirms that the EIS behaviour of Ni-70Cu alloy is considerably reliant on the electrolysis cathodic potential. As the cathodic potential increases, the diameter of two semicircles scrutinized over the Nyquist plots decreases. From **Fig. 6a(inset)** and **Table 3**, the entire charge-transfer resistance, R_f, is calculated at different cathodic potentials which diminishes with the cathodic potential directed to more negative. The R_f of Ni-70Cu alloy cathode lessens from 3.3 Ω (at -1.1 V) to 0.4 Ω (at -1.5 V *vs* SCE), which is confirmed by the decrease of a diameter of the semicircles. With the decrease of the R_f, the cathodic current density greatly increases leading to the high rate of hydrogen evolution reaction. This means that

the augmented rate of H_2 evolution has been obtained due to the improved electrocatalytic activity of the cathode material. The decrease of the charge transfer resistance is reflected in an increase in the current density which confirms that the electrocatalytic activity is achieved via the Ni-70Cu alloy cathode to generate H_2. From Fig. 6 it is palpably that the diameter of both semicircles significantly declines with the cathodic overpotential, demonstrating that both semicircles are associated with the electrode kinetics.[59] As the overpotential grows, the semicircle in the impedance plots develops to be smaller at very elevated cathodic potentials. This is owing to the fact that the adsorption process is enabled and the process of charge transfer controls the impedance response as the potential enlarges. The results reveal that Ni-70Cu is a good candidate for hydrogen production and a promising cathode for practical applications, especially in PBNE . The process is economical and convenient for practical applications. The nanograins contained the small unit cell of Ni-Cu alloys exhibit the high electrocatalytic properties of the cathode surface which is accompanying to the geometrical and physicochemical phenomena. Furthermore, it is recognizable that the mesoporous Ni-70Cu cathode contains the numerous valleys extensively-occupied with the electrolyte, which possesses a significant surface area. This surface is accessible to the electrochemical HER. The bountiful valleys and mesopores are considered the minimum paths for the diffusion to the dissolved hydrogen which enable the instant release of hydrogen and proscribe the accumulation of the hydrogen gas on the surface of the cathode. These mesopores and valleys expand the surface area diminishing the charge transfer resistance for the hydrogen reduction attained via the electroplated Ni-70Cu cathode which is the most appropriate electrocatalyst for the HER. Nanocrystalline cathodes of the 3D and different crystal lattice systems display high electrocatalytic activities for the electrochemical reaction than bulk counterparts [47].Additionally, The kinetics of the HER is

considered the faradaic processes which include the charge transfer and are contingent on the intrinsic electrocatalytic activity of the cathode materials [61]. The electrocatalytic activity of the different alloys for the electrochemical HER is significantly influenced by the synergetic effect of the combination of transition metals owing to their physicochemical properties. The combination of Ni and Cu in the form of Ni-Cu alloys augments appreciably the electrocatalytic activity, for example, electroplated Ni-70Cu cathode. This is because of the modifiable ability to adsorb-desorb the hydrogen through producing the intermediate bonding to hydrogen and the liberating properties [62]. The ideal electrocatalysts for HER possess the free energy of adsorption of the hydrogen is approximated to the thermo-neutral, $\Delta G_H = 0$[47]. Thus, the considerable synergistic effect of the Ni-70Cu cathode improve the HER kinetics. It is praiseworthy to uncover that the electroplated Ni-70Cu alloy cathode is highly stable and it has been used for HER throughout the month without any deterioration of the cathode activity or notable diminution of the rate of hydrogen evolution. Indeed, the electroplated Ni-70Cu alloy cathode attains the minimum hydrogen overpotential and the highest rate of the electrochemical HER which can be utilized via PBNE as new electrocatalyst in the scale of the industry.

.4. Conclusion

The nanocrystalline Ni-Cu alloys were electroplated onto Cu substrate and employed as cathodes for HER in 1.0 M PBNE. Voltammetry and EIS measurements have been implemented to investigate the electrocatalytic activity of the electroplated cathodes towards the HER in 1 M PBS. The prepared catalysts have considerably boosted electrocatalytic activity towards the HER. The increase of the hydrogen evolution activity was related to the Cu content and the huge active surface area. The rate of H_2 production increases as the atomic ratio of Cu in the electroplated cathode increases up to ≈ 70 at%. Layer Ni-Cu alloys of 70 atom% Cu exhibit the

highest electrocatalytic activity for the HER and give the highest rate of H_2 evolution with lowest overpotential. In addition, the polarization and impedance results have displayed that the hydrogen evolution occurs at lowest overpotential on Ni-70Cu compared to the other investigated electrodes in 1M PBNE. The electroplated Ni-70Cu electrode can be considered as a promising cathode for the HER and can be applied as a cathode in industrial water electrolyzer benifiting form the safeer and more sustainable methonds of high efficicncy electrolysis.

References

[1] Wang J, Xu F, Jin H, Chen Y, Wang Y. Non-Noble Metal-based Carbon Composites in Hydrogen Evolution Reaction: Fundamentals to Applications. Adv Mater 2017;29. https://doi.org/10.1002/adma.201605838.

[2] Negem M, Nady H. Electroplated Ni-Cu nanocrystalline alloys and their electrocatalytic activity for hydrogen generation using alkaline solutions. Int J Hydrogen Energy 2017;42:28386–96. https://doi.org/10.1016/j.ijhydene.2017.09.147.

[3] Miao J, Xiao FX, Bin Yang H, Khoo SY, Chen J, Fan Z, et al. Hierarchical Ni-Mo-S nanosheets on carbon fiber cloth: A flexible electrode for efficient hydrogen generation in neutral electrolyte. Sci Adv 2015;1. https://doi.org/10.1126/sciadv.1500259.

[4] Akbayrak M. Efficient Ceria-Supported Rhodium Nanoparticles as an Electrocatalyst for Hydrogen Evolution 2019;166:897–903. https://doi.org/10.1149/2.0701916jes.

[5] Kim H, Kim S. Facile electrochemical preparation of nonprecious Co-Cu alloy catalysts for hydrogen production in proton exchange membrane water electrolysis 2019:19–21. https://doi.org/10.1002/er.5099.

[6] Nørskov JK, Bligaard T, Logadottir A, Kitchin JR, Chen JG, Pandelov S, et al. Trends in the exchange current for hydrogen evolution. J Electrochem Soc 2005;152:0–3. https://doi.org/10.1149/1.1856988.

[7] Nady H, Negem M. Ni-Cu nano-crystalline alloys for efficient electrochemical hydrogen production in acid water. RSC Adv 2016;6. https://doi.org/10.1039/c6ra08348j.

[8] Negem M, Nady H. Electroplated Ni-Cu nanocrystalline alloys and their electrocatalytic activity for hydrogen generation using alkaline solutions. Int J Hydrogen Energy 2017. https://doi.org/10.1016/j.ijhydene.2017.09.147.

[9] Hosseini SR, Ghasemi S, Ghasemi SA. Effect of surfactants on electrocatalytic performance of copper nanoparticles for hydrogen evolution reaction. J Mol Liq 2016;222:1068–75. https://doi.org/10.1016/j.molliq.2016.08.013.

[10] Phillips R, Dunnill CW. Zero gap alkaline electrolysis cell design for renewable energy storage as hydrogen gas. RSC Adv 2016;6:100643–51. https://doi.org/10.1039/c6ra22242k.

[11] Phillips R, Edwards A, Rome B, Jones DR, Dunnill CW. Minimising the ohmic resistance of an alkaline electrolysis cell through effective cell design. Int J Hydrogen Energy 2017;42:23986–94. https://doi.org/10.1016/j.ijhydene.2017.07.184.

[12] Gannon WJF, Dunnill CW. Raney Nickel 2.0: Development of a high-performance bifunctional electrocatalyst. Electrochim Acta 2019;322:134687. https://doi.org/10.1016/j.electacta.2019.134687.

[13] Shi J. On the synergetic catalytic effect in heterogeneous nanocomposite catalysts. Chem Rev 2013;113:2139–81. https://doi.org/10.1021/cr3002752.

[14] Nady H, Negem M. Microstructure and Corrosion Behavior of Electrodeposited NiCo, NiZn and NiCu Nanocrystalline Coatings in Alkaline Solution. Zeitschrift Fur Phys Chemie 2017;231. https://doi.org/10.1515/zpch-2016-0893.

[15] Badawy WA, Nady H, Negem M. Cathodic hydrogen evolution in acidic solutions using electrodeposited nano-crystalline Ni-Co cathodes. Int J Hydrogen Energy 2014;39. https://doi.org/10.1016/j.ijhydene.2014.05.049.

[16] Negem M, Nady H, El-Rabiei MM. Nanocrystalline nickel–cobalt electrocatalysts to generate hydrogen using alkaline solutions as storage fuel for the renewable energy. Int J Hydrogen Energy 2019;44:11411–20. https://doi.org/10.1016/J.IJHYDENE.2019.03.128.

[17] Hu C, Zhang L, Gong J. Recent progress made in the mechanism comprehension and design of electrocatalysts for alkaline water splitting. Energy Environ Sci 2019;12:2620–45. https://doi.org/10.1039/c9ee01202h.

[18] Jakšić MM. Advances in electrocatalysis for hydrogen evolution in the light of the Brewer-Engel valence-bond theory. Int J Hydrogen Energy 1987;12:727–52. https://doi.org/10.1016/0360-3199(87)90090-5.

[19] Jakšić JM, Vojnović M V., Krstajić N V. Kinetic analysis of hydrogen evolution at Ni-Mo alloy electrodes. Electrochim Acta 2000;45:4151–8. https://doi.org/10.1016/S0013-4686(00)00549-1.

[20] Elias L, Cao P, Chitharanjan Hegde A. Magnetoelectrodeposition of Ni-W alloy coatings for enhanced hydrogen evolution reaction. RSC Adv 2016;6:111358–65. https://doi.org/10.1039/c6ra23944g.

[21] Nady H, Negem M. Electroplated Zn–Ni nanocrystalline alloys as an efficient electrocatalyst cathode for the generation of hydrogen fuel in acid medium. Int J Hydrogen Energy 2018;43:4942–50. https://doi.org/10.1016/j.ijhydene.2018.01.119.

[22] Nady H, Negem M. Ni–Cu nano-crystalline alloys for efficient electrochemical hydrogen production in acid water. RSC Adv 2016;6:51111–9. https://doi.org/10.1039/C6RA08348J.

[23] Marceta Kaninski MP, Nikolic VM, Tasic GS, Rakocevic ZL. Electrocatalytic activation of Ni electrode for hydrogen production by electrodeposition of Co and V species. Int J Hydrogen Energy 2009;34:703–9. https://doi.org/10.1016/j.ijhydene.2008.09.024.

[24] Nady H, Negem M. Electroplated Zn-Ni nanocrystalline alloys as an efficient electrocatalyst cathode for the generation of hydrogen fuel in acid medium. Int J Hydrogen Energy 2018. https://doi.org/10.1016/j.ijhydene.2018.01.119.

[25] Badawy WA, Nady H, Negem M. Cathodic hydrogen evolution in acidic solutions using

electrodeposited nano-crystalline Ni-Co cathodes. Int J Hydrogen Energy 2014;39:10824–32. https://doi.org/10.1016/j.ijhydene.2014.05.049.

[26] Martinez S, Metikoš-Huković M, Valek L. Electrocatalytic properties of electrodeposited Ni-15Mo cathodes for the HER in acid solutions: Synergistic electronic effect. J Mol Catal A Chem 2006;245:114–21. https://doi.org/10.1016/j.molcata.2005.09.040.

[27] Solmaz R, Döner A, Kardaş G. The stability of hydrogen evolution activity and corrosion behavior of NiCu coatings with long-term electrolysis in alkaline solution. Int J Hydrogen Energy 2009;34:2089–94. https://doi.org/10.1016/j.ijhydene.2009.01.007.

[28] Stojić DL, Cekić BD, Maksić AD, Kaninski MPM, Miljanić ŠS. Intermetallics as cathode materials in the electrolytic hydrogen production. Int J Hydrogen Energy 2005;30:21–8. https://doi.org/10.1016/j.ijhydene.2004.05.005.

[29] Yu L, Lei T, Nan B, Jiang Y, He Y, Liu CT. Characteristics of a sintered porous Ni-Cu alloy cathode for hydrogen production in a potassium hydroxide solution. Energy 2016;97:498–505. https://doi.org/10.1016/j.energy.2015.12.138.

[30] Ebersbach U, Schwabe K, Ritter K. On the kinetics of the anodic passivation of iron, cobalt and nickel. Electrochim Acta 1967;12:927–38. https://doi.org/10.1016/0013-4686(67)80093-8.

[31] Science C, Britain G, Press P, Engineering M, Science M. THE DISSOLUTION MECHANISM Na2SO 4 SOLUTIONS MONEL 400 IN MONEL 400 alloy has been widely used as a material of construction in sea water environments because of its high corrosion resistance . The corrosion resistance of this alloy has been attributed to 1991;32:799–814.

[32] Okamoto NS and G. Comprehensive Treatise of Electrochemistry. 1981.

[33] Ismail KM, Fathi AM, Badawy WA. Effect of nickel content on the corrosion and passivation of copper-nickel alloys in sodium sulfate solutions. Corrosion 2004;60:795–803. https://doi.org/10.5006/1.3287859.

[34] Ismail KM, Badawy WA. Electrochemical and XPS investigations of cobalt in KOH solutions. J Appl Electrochem 2000;30:1303–11. https://doi.org/10.1023/A:1026560422090.

[35] Pandelov S, Stimming U. Reactivity of monolayers and nano-islands of palladium on Au(1 1 1) with respect to proton reduction. Electrochim Acta 2007;52:5548–55. https://doi.org/10.1016/j.electacta.2007.02.043.

[36] Michalsky R, Zhang YJ, Peterson AA. Trends in the hydrogen evolution activity of metal carbide catalysts. ACS Catal 2014;4:1274–8. https://doi.org/10.1021/cs500056u.

[37] Mahmood N, Yao Y, Zhang JW, Pan L, Zhang X, Zou JJ. Electrocatalysts for Hydrogen Evolution in Alkaline Electrolytes: Mechanisms, Challenges, and Prospective Solutions. Adv Sci 2018;5. https://doi.org/10.1002/advs.201700464.

[38] Conway BE, Tilak B V. Interfacial processes involving electrocatalytic evolution and oxidation of H2, and the role of chemisorbed H. Electrochim Acta 2002;47:3571–94. https://doi.org/10.1016/S0013-4686(02)00329-8.

[39] Liu Y, Yu H, Quan X, Chen S, Zhao H, Zhang Y. Efficient and durable hydrogen evolution electrocatalyst based on nonmetallic nitrogen doped hexagonal carbon. Sci Rep 2014;4:1–6. https://doi.org/10.1038/srep06843.

[40] Liu B, Zhang L, Xiong W, Ma M. Cobalt-Nanocrystal-Assembled Hollow Nanoparticles for Electrocatalytic Hydrogen Generation from Neutral-pH Water. Angew Chemie - Int Ed 2016;55:6725–9. https://doi.org/10.1002/anie.201601367.

[41] Gupta S, Patel N, Fernandes R, Kadrekar R, Dashora A, Yadav AK, et al. Co-Ni-B nanocatalyst for efficient hydrogen evolution reaction in wide pH range. Appl Catal B Environ 2016;192:126–33. https://doi.org/10.1016/j.apcatb.2016.03.032.

[42] Gupta S, Patel N, Miotello A, Kothari DC. Cobalt-Boride: An efficient and robust electrocatalyst for Hydrogen Evolution Reaction. J Power Sources 2015;279:620–5. https://doi.org/10.1016/j.jpowsour.2015.01.009.

[43] Kuang Y, Feng G, Li P, Bi Y, Li Y, Sun X. Single-Crystalline Ultrathin Nickel Nanosheets Array from in Situ Topotactic Reduction for Active and Stable Electrocatalysis. Angew Chemie - Int Ed 2016;55:693–7. https://doi.org/10.1002/anie.201509616.

[44] Zhang Y, Li P, Yang X, Fa W, Ge S. High-efficiency and stable alloyed nickel based electrodes for hydrogen evolution by seawater splitting. J Alloys Compd 2018;732:248–56. https://doi.org/10.1016/j.jallcom.2017.10.194.

[45] Niu X, Tang Q, He B, Yang P. Robust and stable ruthenium alloy electrocatalysts for hydrogen evolution by seawater splitting. Electrochim Acta 2016;208:180–7. https://doi.org/10.1016/j.electacta.2016.04.184.

[46] Li H, Tang Q, He B, Yang P. Robust electrocatalysts from an alloyed Pt-Ru-M (M = Cr, Fe, Co, Ni, Mo)-decorated Ti mesh for hydrogen evolution by seawater splitting. J Mater Chem A 2016;4:6513–20. https://doi.org/10.1039/c6ta00785f.

[47] Zheng J. Seawater splitting for high-efficiency hydrogen evolution by alloyed PtNi x electrocatalysts. Appl Surf Sci 2017;413:360–5. https://doi.org/10.1016/j.apsusc.2017.03.285.

[48] Gomez Vidales A, Omanovic S. Evaluation of nickel-molybdenum-oxides as cathodes for hydrogen evolution by water electrolysis in acidic, alkaline, and neutral media. Electrochim Acta 2018;262:115–23. https://doi.org/10.1016/j.electacta.2018.01.007.

[49] Liang Y, Liu Q, Asiri AM, Sun X, Luo Y. Self-supported FeP nanorod arrays: A cost-effective 3D hydrogen evolution cathode with high catalytic activity. ACS Catal 2014;4:4065–9. https://doi.org/10.1021/cs501106g.

[50] Tran PD, Nguyen M, Pramana SS, Bhattacharjee A, Chiam SY, Fize J, et al. Copper molybdenum sulfide: A new efficient electrocatalyst for hydrogen production from water. Energy Environ Sci 2012;5:8912–6. https://doi.org/10.1039/c2ee22611a.

[51] hydrogen evolution reaction with low overpotential in neutral solution A highly active and robust copper-based electrocatalyst toward hydrogen evolution reaction with low overpotential in neutral solution 2016. https://doi.org/10.1021/acsami.6b09975.

[52] Zhao Y, Tang Q, He B, Yang P. Carbide decorated carbon nanotube electrocatalyst for high-efficiency hydrogen evolution from seawater. RSC Adv 2016;6:93267–74. https://doi.org/10.1039/c6ra17839a.

[53] Zhao J, Tran PD, Chen Y, Loo JSC, Barber J, Xu ZJ. Achieving High Electrocatalytic Efficiency on Copper: A Low-Cost Alternative to Platinum for Hydrogen Generation in Water. ACS Catal

2015;5:4115–20. https://doi.org/10.1021/acscatal.5b00556.

[54] Hou Y, Zhang B, Wen Z, Cui S, Guo X, He Z, et al. A 3D hybrid of layered MoS2/nitrogen-doped graphene nanosheet aerogels: An effective catalyst for hydrogen evolution in microbial electrolysis cells. J Mater Chem A 2014;2:13795–800. https://doi.org/10.1039/c4ta02254h.

[55] Gao S, Li GD, Liu Y, Chen H, Feng LL, Wang Y, et al. Electrocatalytic H2 production from seawater over Co, N-codoped nanocarbons. Nanoscale 2015;7:2306–16. https://doi.org/10.1039/c4nr04924a.

[56] Pu Z, Wei S, Chen Z, Mu S. Flexible molybdenum phosphide nanosheet array electrodes for hydrogen evolution reaction in a wide pH range. Appl Catal B Environ 2016;196:193–8. https://doi.org/10.1016/j.apcatb.2016.05.027.

[57] Mo Q, Zhang W, He L, Yu X, Gao Q. Bimetallic Ni2-xCoxP/N-doped carbon nanofibers: Solid-solution-alloy engineering toward efficient hydrogen evolution. Appl Catal B Environ 2019;244:620–7. https://doi.org/10.1016/j.apcatb.2018.11.083.

[58] Krstajić N V., Jović VD, Gajić-Krstajić L, Jović BM, Antozzi AL, Martelli GN. Electrodeposition of Ni-Mo alloy coatings and their characterization as cathodes for hydrogen evolution in sodium hydroxide solution. Int J Hydrogen Energy 2008;33:3676–87. https://doi.org/10.1016/j.ijhydene.2008.04.039.

[59] Birry L, Lasia A. Studies of the hydrogen evolution reaction on Raney nickel-molybdenum electrodes. J Appl Electrochem 2004;34:735–49. https://doi.org/10.1023/B:JACH.0000031161.26544.6a.

[60] Chen L, Lasia A. Study of the Kinetics of Hydrogen Evolution Reaction on Nickel-Zinc Powder Electrodes. J Electrochem Soc 1992;139:3214–9. https://doi.org/10.1149/1.2069055.

[61] Los P, Lasia A, Ménard H, Brossard L. Impedance studies of porous lanthanum-phosphate-bonded nickel electrodes in concentrated sodium hydroxide solution. J Electroanal Chem 1993;360:101–18. https://doi.org/10.1016/0022-0728(93)87007-I.

[62] Greeley J, Jaramillo TF, Bonde J, Chorkendorff I, Nørskov JK. Computational high-throughput screening of electrocatalytic materials for hydrogen evolution. Nat Mater 2006;5:909–13. https://doi.org/10.1038/nmat1752.

Table 1- The electrochemical data determined from cathodic current-potential curves at different overpotentials.

Cathode	$-bc$ / mV dec^{-1}	η_{10} / mV	η_{100} / mV	$i_{-1.1}$/ mA cm^{-2}	$i_{-1.2}$/ mA cm^{-2}	$i_{-1.4}$/ mA cm^{-2}
bulk Ni	123	468	1118	8.3	18.2	46
ed. Ni	114	339	667	30.7	58	133
Ed. Cu	133	345	676	38	62	122
Ni-24Cu	149	333	606	44.2	78	156
Ni-59Cu	138	301	612	50.4	78	147
Ni-70Cu	109	284	504	77.2	118	216
Ni-85Cu	116	297	589	53	86	155

Table 2- Comparison of HER performance with representative HER electrocatalysts in different media.

Coating	Electrolyte	Over potential η_{10} (**mV vs. RHE**)	Tafel slope (mV dec^{-1})	Reference
Co-B NPs	0.5M PBS	-251	75	[42]
CoNiB	0.5M PBS	-170	51	[41]
Co-HNP	1.0M PBS	-85	38	[40]
Ni-NSA	0.1M KOH	~ -120	114	[43]
Ti/NiCu	seawater	/	170	[44]
Ti/NiCo	seawater	/	167	[44]
Ti/NiMo	seawater	/	188	[44]
RuCo	seawater	∼-300	107	[45]
Pt–Ru–Cr	seawater	-286	126	[46]
Pt–Ru–Fe	seawater	-248	122	[46]
Pt–Ru–Co	seawater	-222	110	[46]
Pt–Ru–Ni	seawater	-206	104	[46]
Pt–Ru–Mo	seawater	-196	100	[46]
$PtNi_5$	seawater	/	119	[47]
$PtNi_{10}$	seawater	/	148	[47]
$Ni_{0.8}Mo_{0.2}Ox$	0.6M NaCl	/	152 ± 9	[48]
NiOx	0.6M NaCl	/	173 ± 15	[48]
FeP/CC	1 M PBS	-120	70	[49]
Cu_2MoS_4	0.1 M PBS	-620 (η_2)	/	[50]
Cu(II) oxime	0.5 M PBS	-120 (η_1)	63	[51]
Nickel foam	seawater	-695	262	[52]
Commercial CNT	seawater	- 600	/	[53]
Co_3Mo_3C/CNT	seawater	- 124	249	[53]
3D MoS_2/N-GAs	0.1 M PBS	-261	230	[54]
Co,N-doped nanocarbons	seawater	-240	159	[55]
MoP NA/CC	1 M PBS	-187	94	[56]
$Ni_{1.67}Co_{0.33}P$	1 M PBS	-326	125	[57]
Ni-70Cu	1 M PBS	-284	109	This work

Table 3- The electrochemical data determined from cathodic current-potential curves at different overpotentials.

Cathode	E (mV) *vs* SCE	R_s/ Ω	R_1/ Ω cm^2	C_{dl}/ mF cm^{-2}	R_2/ Ω cm^2	C_p/ mF cm^{-2}	R_f (R1+R2)
ed. Ni	-1.0	1.4	3.5	0.365	5.0	1.28	8.5
ed. Cu	-1.0	1.02	0.32	12.45	4.2	152.8	4.52
Ni-70Cu	-1.0	1.0	1.6	2.5	1.7	36.8	3.3
Ni-70Cu	-1.05	1.1	1.34	2.96	1.4	55.5	2.74
Ni-70Cu	-1.1	1.1	0.86	2.92	1.23	16.3	2.09
Ni-70Cu	-1.2	1.1	0.44	2.27	0.73	27.6	1.17
Ni-70Cu	-1.3	1.0	0.45	2.8	0.42	7.5	0.87
Ni-70Cu	-1.4	1.03	0.24	2.62	0.2	94.0	0.44
Ni-70Cu	-1.5	1.0	0.2	2.2	0.2	7.1	0.4

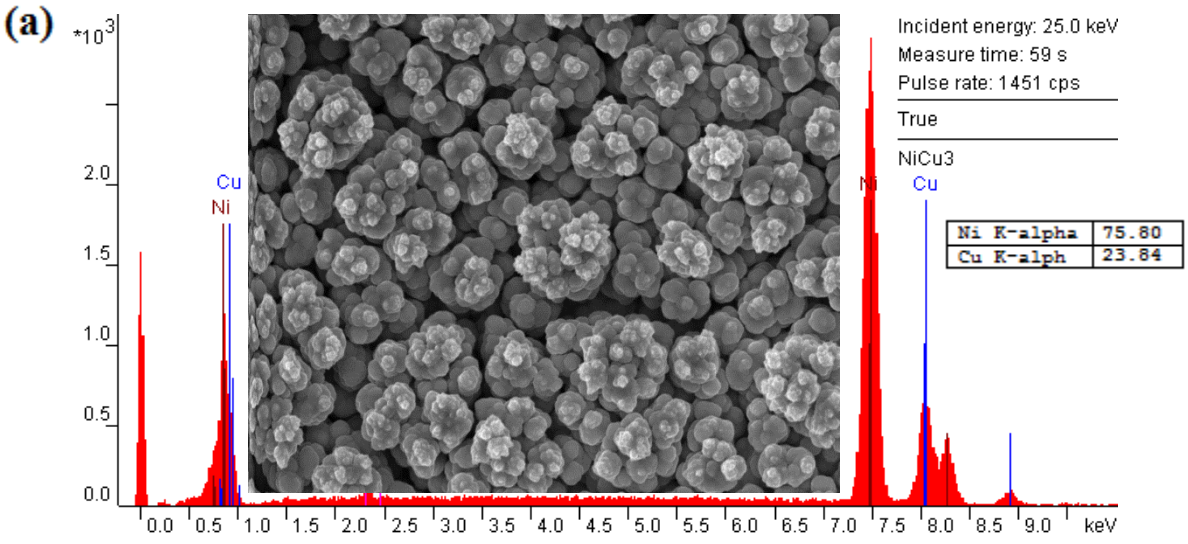

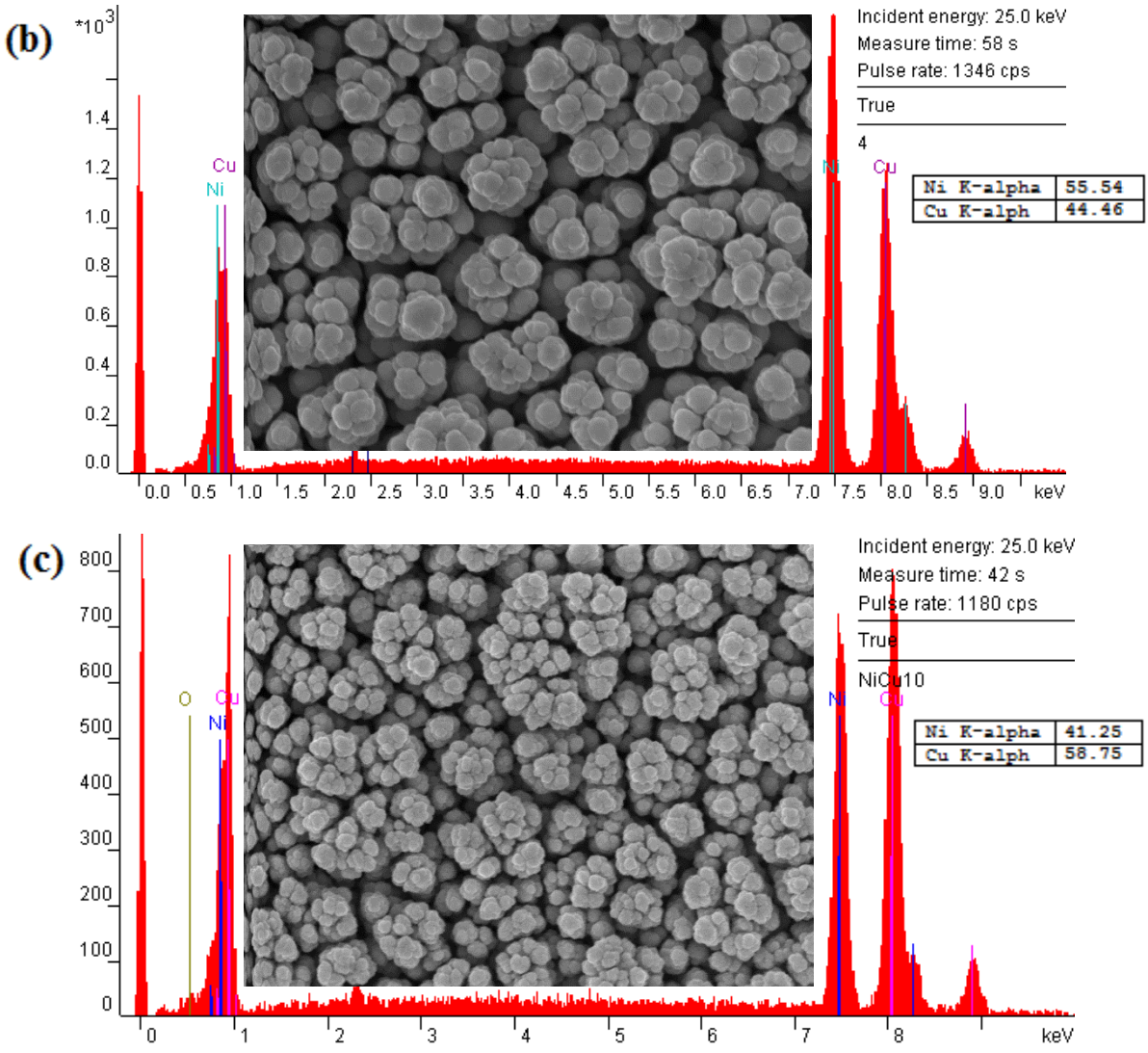

Fig. 1- SEM/EDX analyses of different Ni-Cu nanocrystalline coatings.

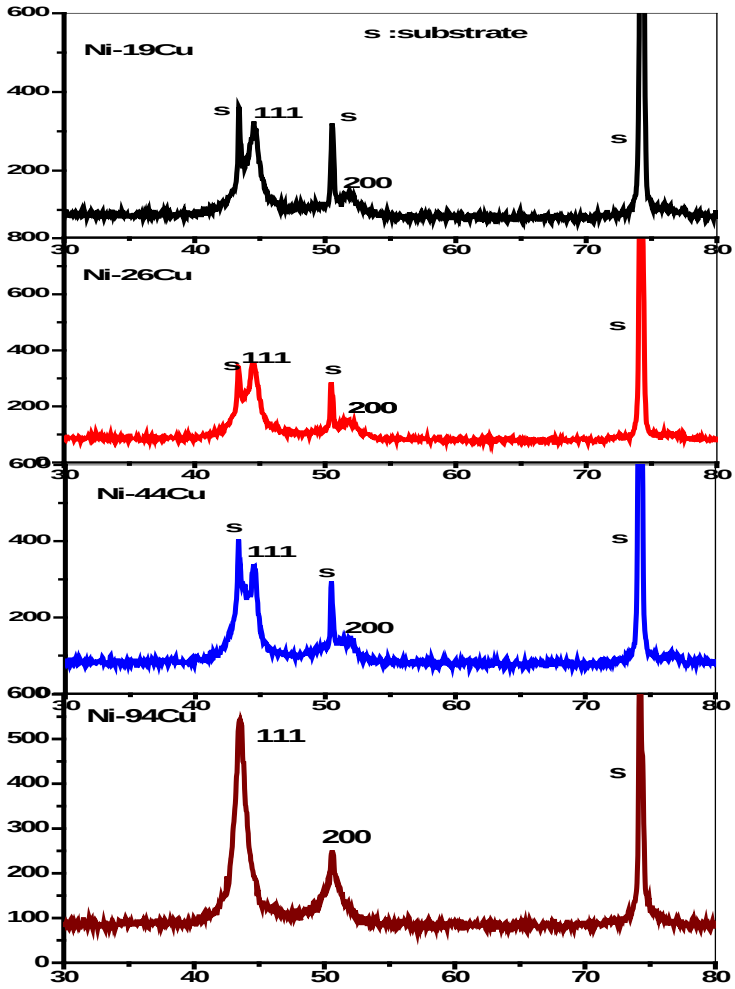

Figure 2- XRD patterns of nanocrystalline Ni-Cu bimetals obtained via gluconate bath using conventional ultrasound waves.

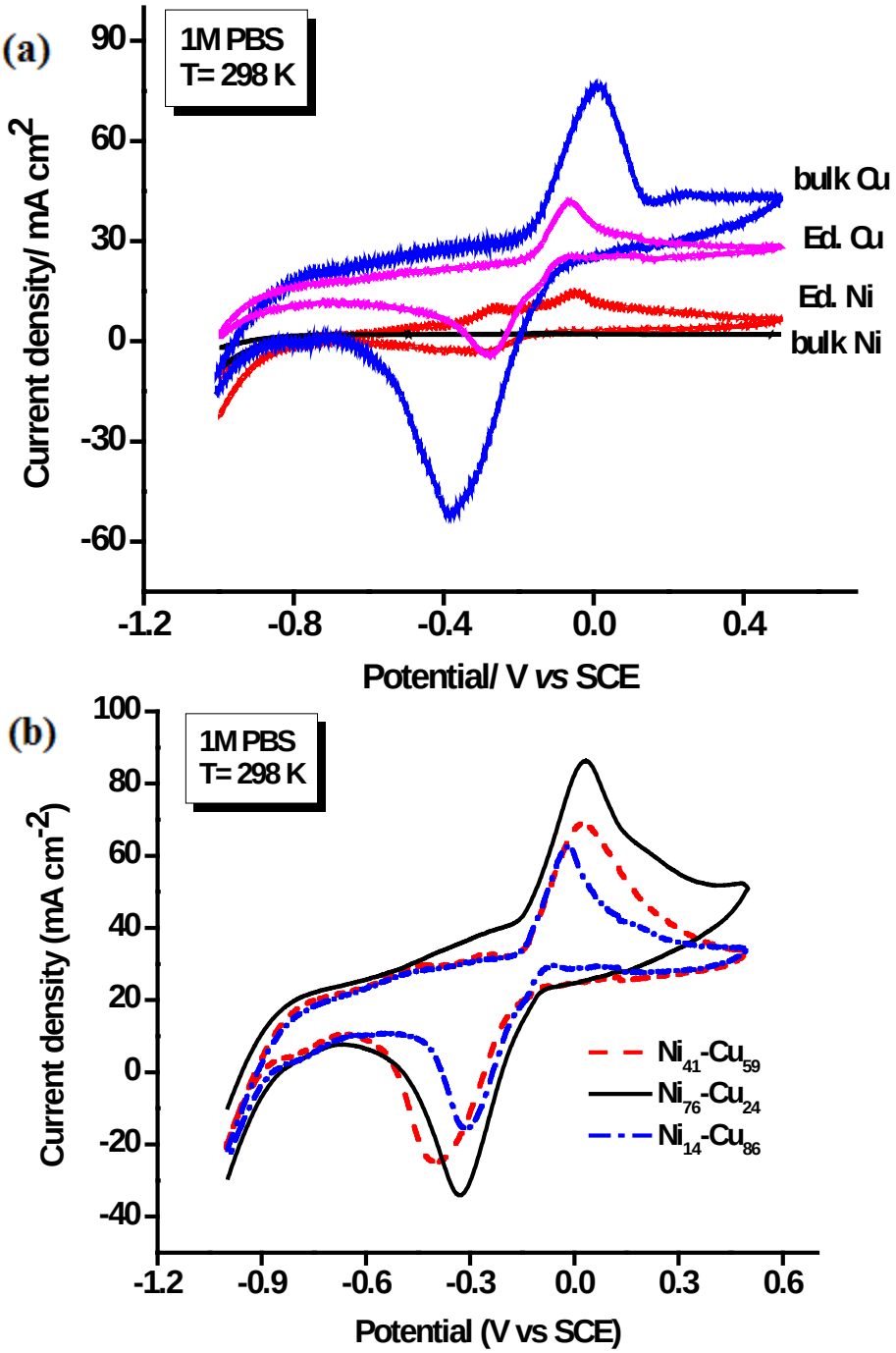

Fig. 3 - Cyclic voltammetry curves of Ni-Cu nanocrystals and single metal.

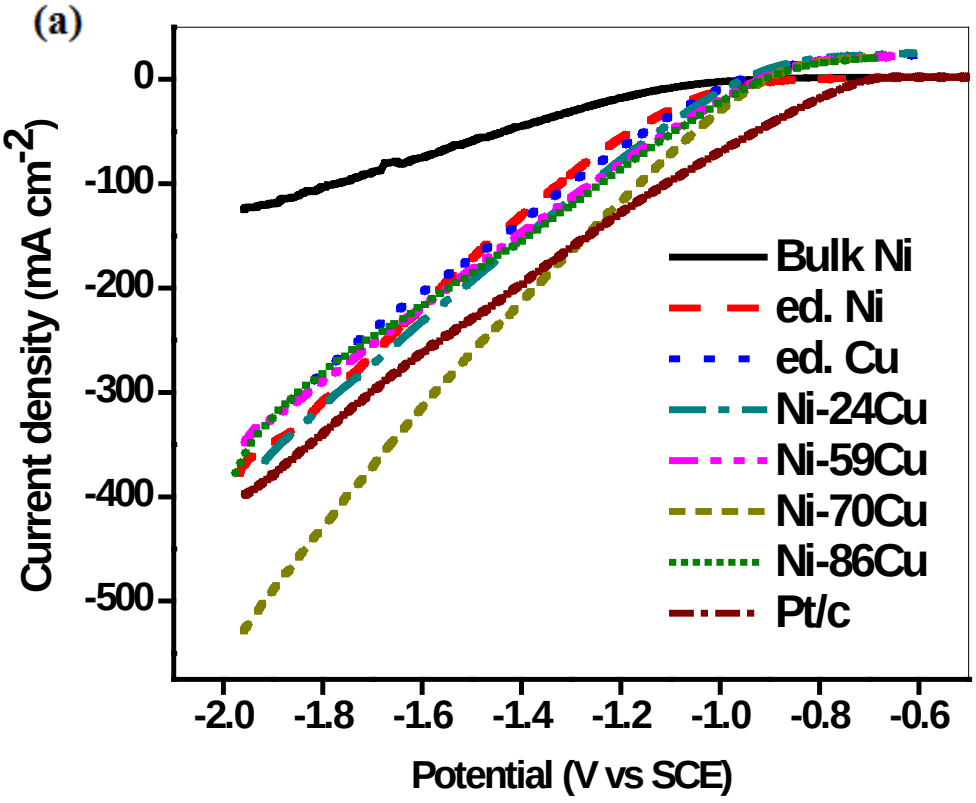
(a)
Current density (mA cm-2)
0
-100
-200
-300
-400
-500
-2.0
-1.8
-1.6
-1.4
-1.2
-1.0
-0.8
-0.6
Potential (V vs SCE)
Bulk Ni
ed. Ni
ed. Cu
Ni-24Cu
Ni-59Cu
Ni-70Cu
Ni-86Cu
Pt/c

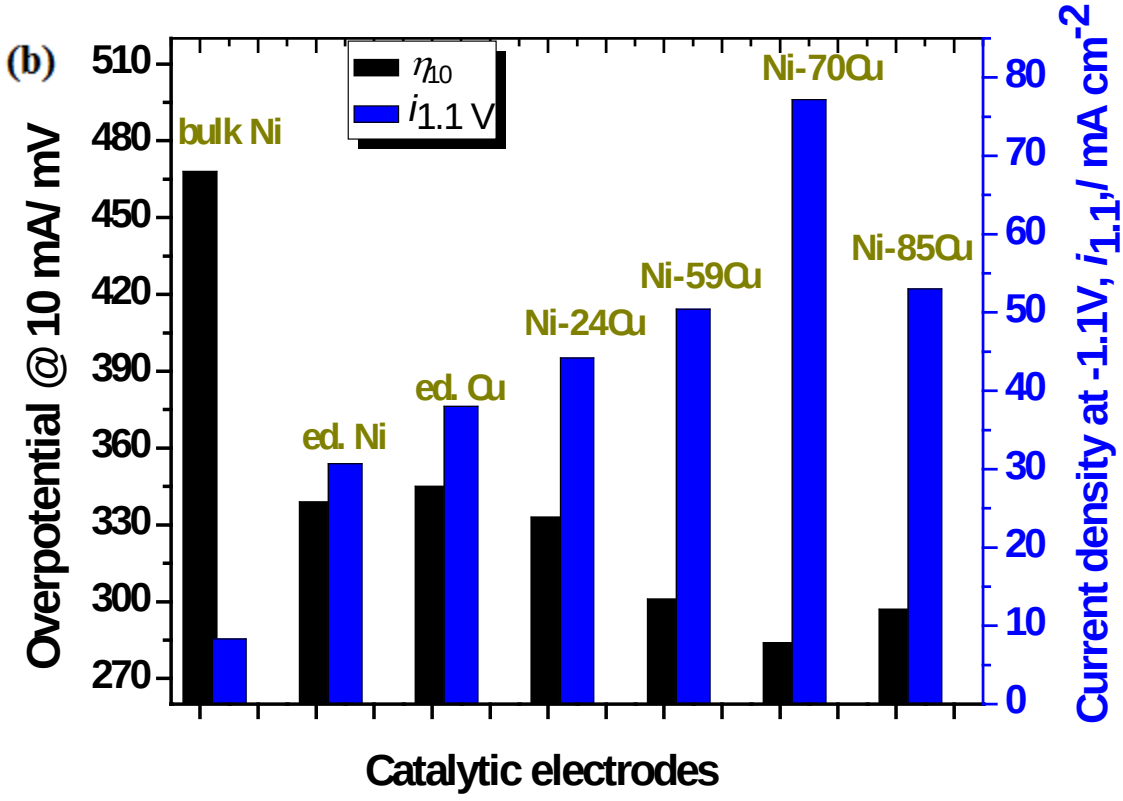
(b)
Overpotential @ 10 mA/ mV
510
480
450
420
390
360
330
300
270
Current density at -1.1V, i1.1/ mA cm-2
80
70
60
50
40
30
20
10
0
η10
i1.1 V
bulk Ni
ed. Ni
ed. Cu
Ni-24Cu
Ni-59Cu
Ni-70Cu
Ni-85Cu
Catalytic electrodes

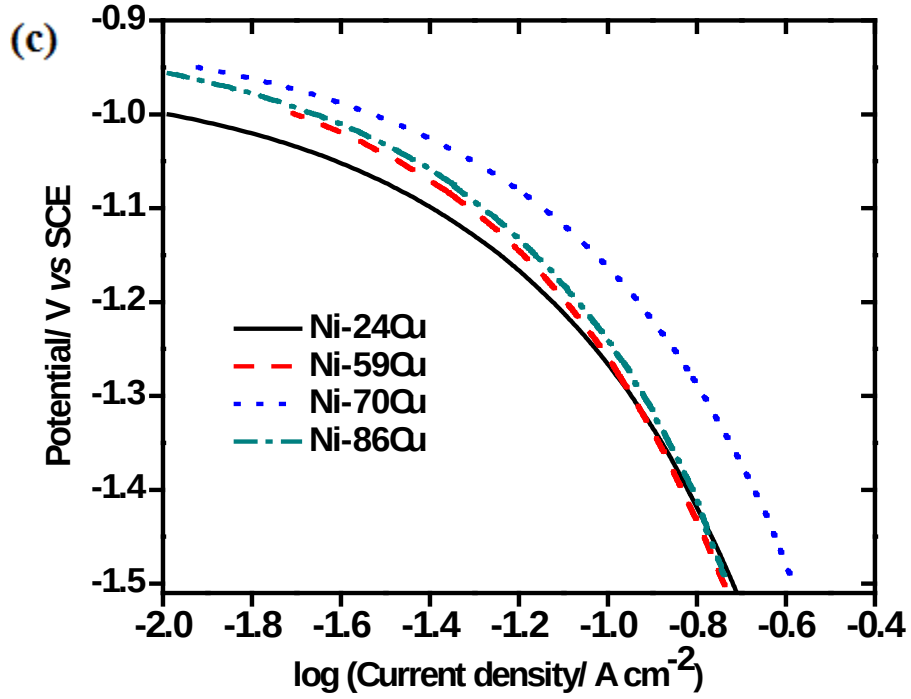

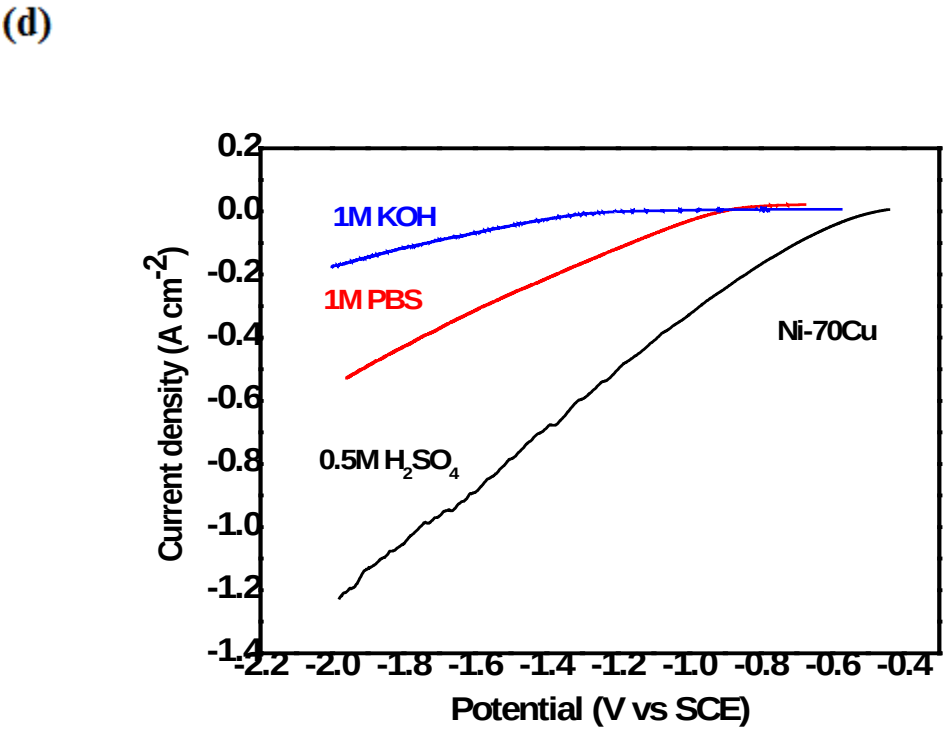

Fig. 4- (a) Polarization curves of bulk Ni, ed. Ni, ed. Cu, Ni-24Cu, Ni-59Cu, Ni-70Cu, Ni-85Cu and Pt/C in 1M PBS solution, (b) Overpotential values at current density of 10 mA/cm^{-2} (η_{10}) and the current density at 1.1 V vs. SCE ($i_{1.1\ V}$) for the different cathodes, (c) Tafel plots of Ni-24Cu, Ni-59Cu, Ni-70Cu, Ni-85Cu coatings. (d) Polarization curves of Ni-70Cu coating in 0.5M H_2SO_4, 1M KOH, and 1M PBS solutions.

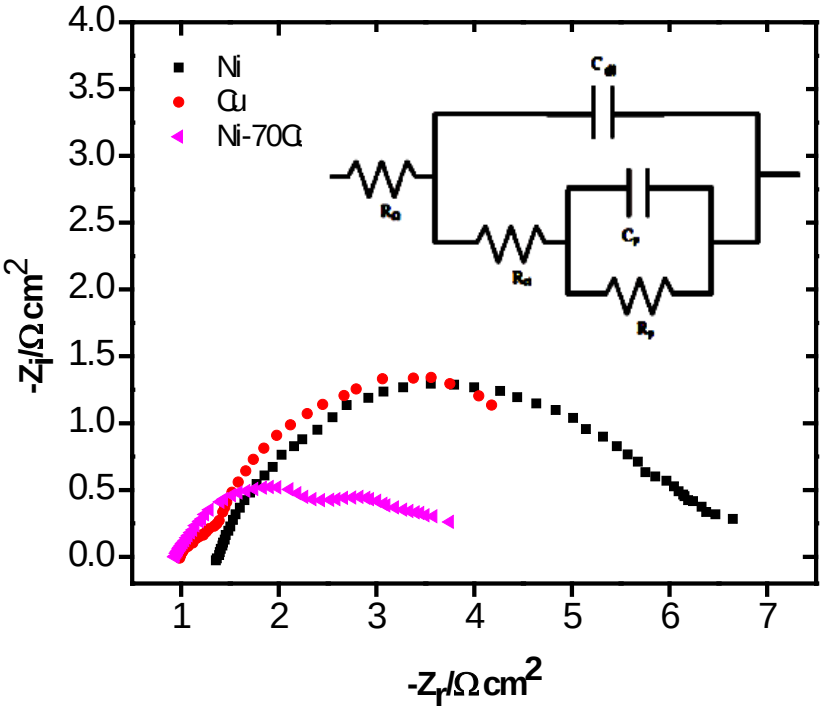

Fig.5- Nyquist plots of Ni, Cu and Ni-Cu coatings at 1.0V (*vs* SCE), inset in (a): the corresponding equivalent circuit model.

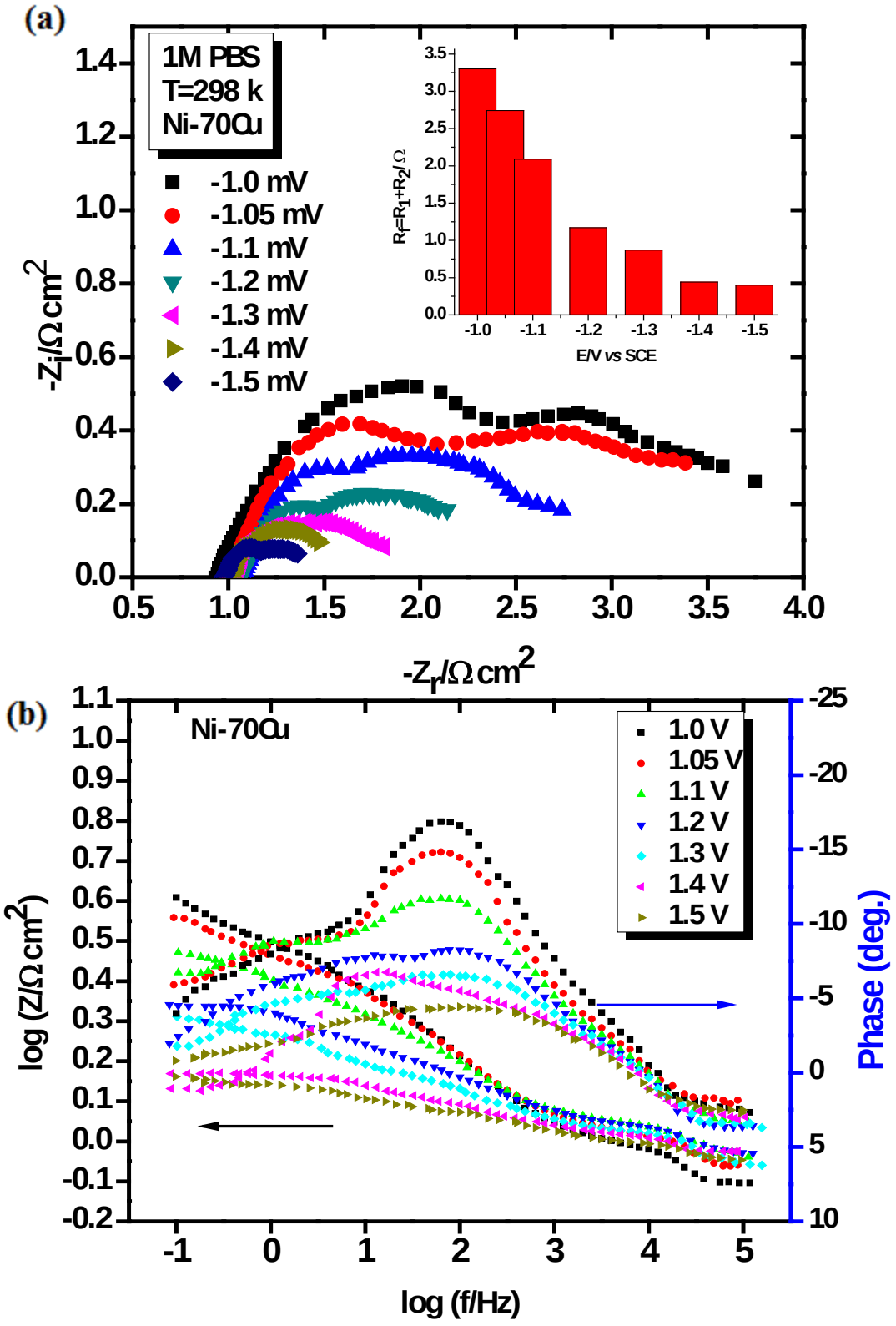

Fig.6- Nyquist (a) and Bode (b) diagrams for nanocrystalline Ni-70Cu at different potentials.